

Spectra of identified hadrons with the ALICE detector in pp and Pb–Pb collisions at the LHC

Roberto Preghenella (for the ALICE Collaboration)

Centro Studi e Ricerche e Museo Storico della Fisica “Enrico Fermi”, Rome, Italy

Dipartimento di Fisica dell’Università and Sezione INFN, Bologna, Italy

E-mail: preghenella@bo.infn.it

Abstract

The measurement of identified charged-hadron production at mid-rapidity ($|y| < 0.5$) performed with the ALICE experiment at the LHC is presented for pp collisions at $\sqrt{s} = 900$ GeV and 7 TeV and for Pb–Pb collisions at $\sqrt{s_{NN}} = 2.76$ TeV. Transverse momentum spectra of π^\pm , K^\pm , p, \bar{p} and multi-strange baryons are measured over a wide momentum range using the dE/dx , the time-of-flight and topological particle-identification techniques. In this report, the particle-identification detectors and techniques, as well as the achieved performance, are shortly reviewed. Proton-proton results on particle production yields, spectral shapes and particle ratios are presented as a function of the collision energy and compared to previous experiments and commonly-used Monte Carlo models. Particle spectra, yields and ratios in Pb–Pb are measured as a function of the collision centrality and the results are compared with published RHIC data in Au–Au collisions at $\sqrt{s_{NN}} = 200$ GeV and predictions for the LHC.

1 Introduction

ALICE (A Large Ion Collider Experiment) is a general-purpose heavy-ion experiment at the CERN LHC (Large Hadron Collider) aimed at studying the physics of strongly-interacting matter and the quark–gluon plasma. A unique design has been adopted for the ALICE detector to fulfill tracking and particle-identification requirements [1]. Thanks to these features the experiment is able to identify hadrons in a wide momentum range by combining different detecting systems and techniques, as discussed in Section 2. Results on hadron spectra and yields at mid-rapidity are presented in Section 3 for pp collisions at $\sqrt{s} = 900$ GeV and 7 TeV and in Section 4 for Pb–Pb collisions at $\sqrt{s_{NN}} = 2.76$ TeV.

2 Particle identification

In this section the particle-identification (PID) detectors relevant for the analyses presented in this paper are briefly discussed, namely the *Inner Tracking*

System (ITS), the *Time-Projection Chamber* (TPC) and the *Time-Of-Flight* detector (TOF). A detailed review of the ALICE detector and of its PID capabilities can be found in [1]. The ITS is a six-layer silicon detector located at radii between 4 and 43 cm. Four of the six layers provide dE/dx measurements and are used for hadron identification in the non-relativistic ($1/\beta^2$) region. Moreover, using the ITS as a standalone tracker enables one to reconstruct and identify low-momentum hadrons not reaching the main tracking systems. The TPC is the main central-barrel tracking detector of ALICE and provides three-dimensional hit information and specific energy-loss measurements with up to 159 samples. With the measured particle momentum and $\langle dE/dx \rangle$ the hadron type can be determined by comparing the measurements against the Bethe-Bloch expectation. The TOF detector is a large-area array of Multigap Resistive Plate Chambers (MRPC) and covers the central pseudorapidity region ($|\eta| < 0.9$, full azimuth). Hadron identification is performed by matching momentum and trajectory-length measurements performed by the tracking system with the time-of-flight information provided by the TOF system. The total time-of-flight resolution is about 85 ps in Pb–Pb collisions and it is determined by the time resolution of the detector itself and by the start-time resolution.

The transverse momentum spectra of primary π^\pm , K^\pm , p and \bar{p} are measured at mid-rapidity ($|y| < 0.5$) combining the techniques and detectors described above. Primary hadrons are defined as prompt particles produced in the collision and all decay products, except products from weak decay of strange particles. The contribution from the feed-down of weakly-decaying particles to π^\pm , p and \bar{p} and from protons from material are subtracted by fitting the data using Monte Carlo templates of the DCA¹ distributions. Particles can also be identified in ALICE via their characteristics decay topology or invariant mass fits. This, combined with the direct identification of the decay daughters allows to reconstruct weakly-decaying particles and hadronic resonances with an improved signal-to-background ratio.

3 Results in pp collisions

The transverse momentum spectra of primary π^\pm , K^\pm , p and \bar{p} are measured in minimum-bias pp collisions at $\sqrt{s} = 900$ GeV and 7 TeV. The measurements performed at $\sqrt{s} = 900$ GeV and the details of the analysis are already published in [2]. The results of the analysis performed at $\sqrt{s} = 7$ TeV together with the corresponding fits to the data are shown in Figure 1 (left) for negative hadrons. The Lévy-Tsallis [3] parameterization provides a good description of the spectral shapes at both energies and allows to extrapolate the spectra outside the measured p_T range to compute integrated yields dN/dy and average transverse momenta $\langle p_T \rangle$. Figure 1 (right) compares $\langle p_T \rangle$ at different energies and colliding systems which is observed to rise with increasing \sqrt{s} . The ratios K/π and p/π as a function of p_T are shown in Figure 2 comparing measurements at $\sqrt{s} = 900$ GeV and 7 TeV. Both particle ratios do not show evident energy dependence. A comparison with Monte Carlo generators shows that K/π ratio

¹Distance of Closest Approach to the reconstructed primary vertex.

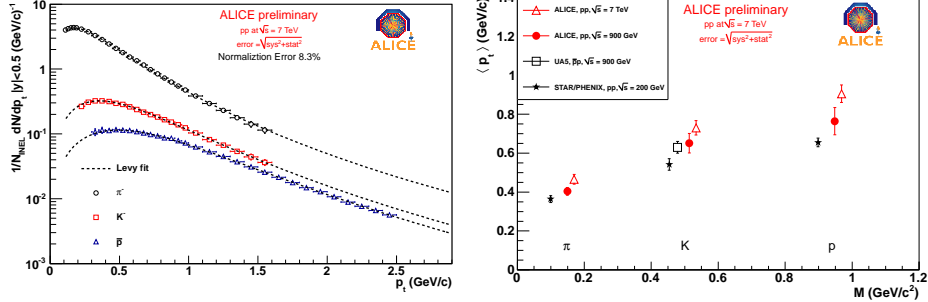


Figure 1: Transverse momentum spectra of primary π^- , K^- , \bar{p} and corresponding fits in pp collisions at $\sqrt{s} = 7$ TeV (left). Mean p_T as function of the hadron mass (right).

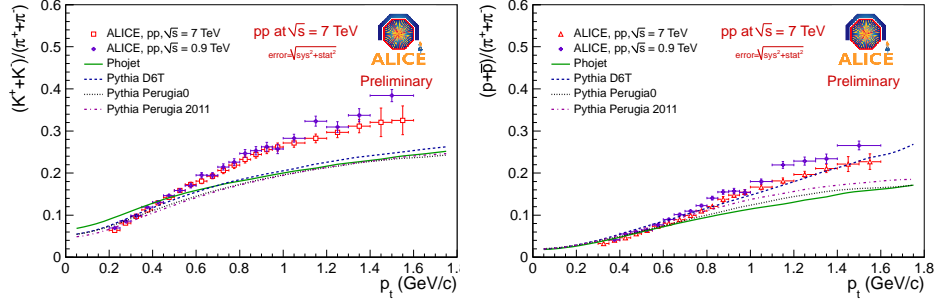


Figure 2: K/π (left) and p/π (right) production ratios as a function of p_T measured in pp collisions at $\sqrt{s} = 900$ GeV and 7 TeV compared to various Monte Carlo models at $\sqrt{s} = 7$ TeV.

is underestimated at high- p_T by recent PYTHIA tunes. The same holds for p/π ratio, though a better agreement with the data is observed for PYTHIA D6T. Figure 3 shows the integrated production ratios K/π and p/π as a function of \sqrt{s} . They are observed to be rather independent of the collision energy from 900 GeV to 7 TeV. Moreover, for these energies there are no difference between p/π^+ and \bar{p}/π^- , hence the baryon/antibaryon asymmetry vanishes at LHC energies as already reported in [4] leading to a constant value of about 0.05.

Measurements of the production of multi-strange baryons $\Xi \rightarrow \Lambda + \pi \rightarrow p + \pi + \pi$ and $\Omega \rightarrow \Lambda + K \rightarrow p + \pi + K$ were also reported at this conference and in [5]. The Ξ^- and Ω^- baryon and their antiparticle spectra are shown in Figure 4 (left, top panel) with the corresponding Lévy-Tsallis fits. When compared to Monte Carlo event generators multi-strange production is under-predicted by various PYTHIA tunes, though the most-recent Perugia-2011 tune shows an overall better agreement with the data reported in Figure 4 (left, bottom panel). The p_t -integrated dN/dy and $\langle p_t \rangle$ are reported in Figure 4

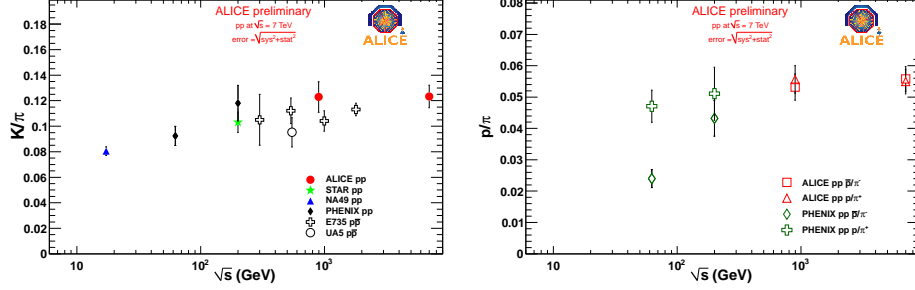


Figure 3: K/π (left) and p/π (right) integrated production ratios as a function of \sqrt{s} .

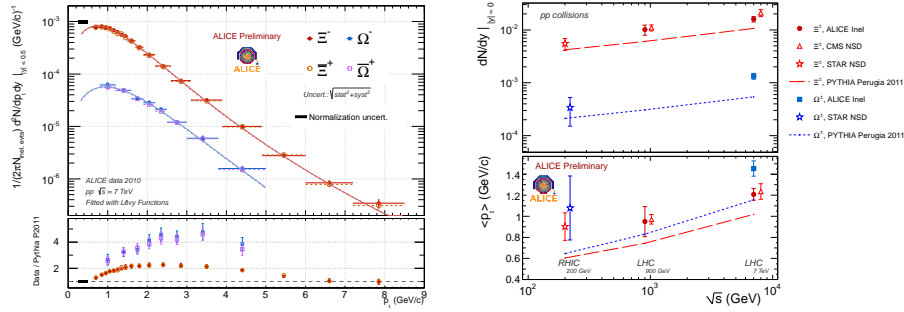


Figure 4: Ξ^- and Ω^- baryon and their antiparticle spectra (left, top panel) and the comparison to PYTHIA Perugia 2011 Monte Carlo (left, bottom panel). dN/dy (right, top panel) and $\langle p_t \rangle$ (right, bottom panel) of Ξ^\pm and Ω^\pm as a function of collision energy.

(right) as a function of the collision energy together with STAR [6] and CMS [7] results. They are observed to increase with collision energy and due to the precision of the ALICE measurements a significant separation between the $\langle p_t \rangle$ of Ξ^\pm and Ω^\pm is observed in proton-proton collisions at 7 TeV.

4 Results in Pb–Pb collisions

Hadron spectra are measured in several centrality classes (see [8] for details on centrality selection) from 100 MeV/c up to 3 GeV/c for pions, from 200 MeV/c up to 2 GeV/c for kaons and from 300 MeV/c up to 3 GeV/c for protons and antiprotons. Individual fits to the data are performed following a blast-wave parameterization [9] to extrapolate the spectra outside the measured p_T range. The measured spectra and corresponding fits are shown in Figure 5 for primary π^- (top left), K^- (top right) and \bar{p} (bottom left). Average transverse momenta $\langle p_T \rangle$ and integrated production yields dN/dy are obtained using the measured data points and the extrapolation. Antiparticle/particle integrated production

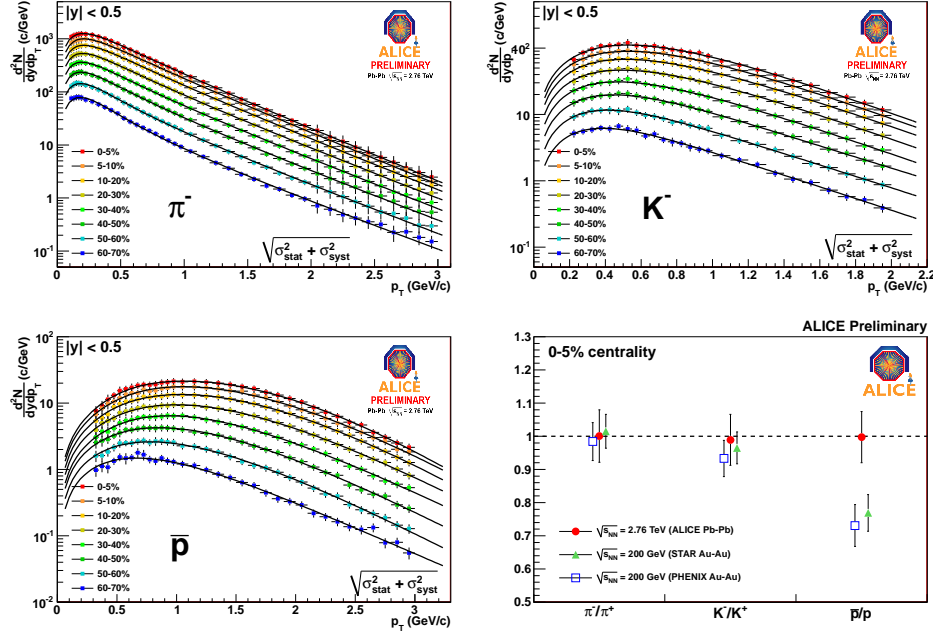


Figure 5: Transverse momentum spectra of primary π^- (top left), K^- (top right), \bar{p} (bottom left) and corresponding fits in Pb-Pb collisions at $\sqrt{s_{NN}} = 2.76$ TeV. Antiparticle/particle production ratios in the 0-5% most central collisions (bottom right).

ratios are observed to be consistent with unity for all hadron species in all centrality classes suggesting that the baryo-chemical potential μ_B is close to zero as expected at LHC energies. Figure 5 (bottom right) compares ALICE results with RHIC Au-Au collisions at $\sqrt{s_{NN}} = 200$ GeV [10] for the 0-5% most central collisions.

The p_T -integrated K^-/π^- and \bar{p}/π^- ratios are shown in Figure 6 as a function of the charged-particle density $dN_{ch}/d\eta$ [8] and are compared with RHIC data at $\sqrt{s_{NN}} = 200$ GeV and ALICE proton-proton results at $\sqrt{s} = 7$ TeV. K^-/π^- production nicely follows the trend measured by STAR. \bar{p}/π^- results are similar to previous measurements performed by PHENIX and BRAHMS (proton measurements reported by STAR are inclusive). Finally, the \bar{p}/π^- ratio measured at the LHC (~ 0.05) is significantly lower than the value expected from statistical model predictions (~ 0.07 - 0.09) with a chemical freeze-out temperature of $T_{ch} = 160 - 170$ MeV at the LHC [11].

The measured hadron $\langle p_T \rangle$'s are shown in Figure 7 (left) as a function of $dN_{ch}/d\eta$ for π^- , K^- and \bar{p} and are compared to STAR results in Au-Au collisions at $\sqrt{s_{NN}} = 200$ GeV. The measured spectra at the LHC are observed to be harder than at RHIC for similar $dN_{ch}/d\eta$. A detailed study of the spectral shapes has been done in order to give a quantitative estimate of the thermal

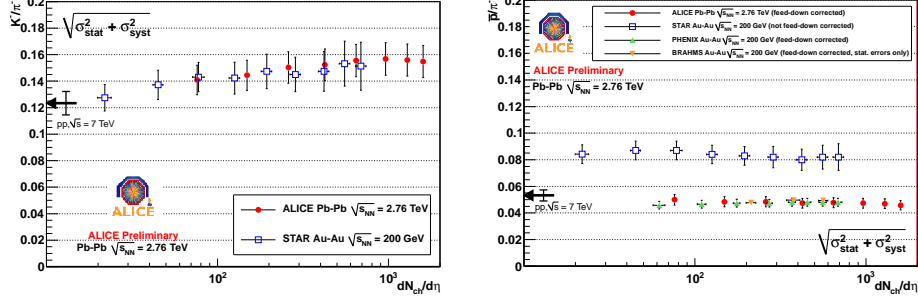


Figure 6: K^-/π^- (left) and \bar{p}/π^- (right) production ratios as a function of $dN_{ch}/d\eta$ in Pb–Pb collisions at $\sqrt{s_{NN}} = 2.76$ TeV compared to RHIC data.

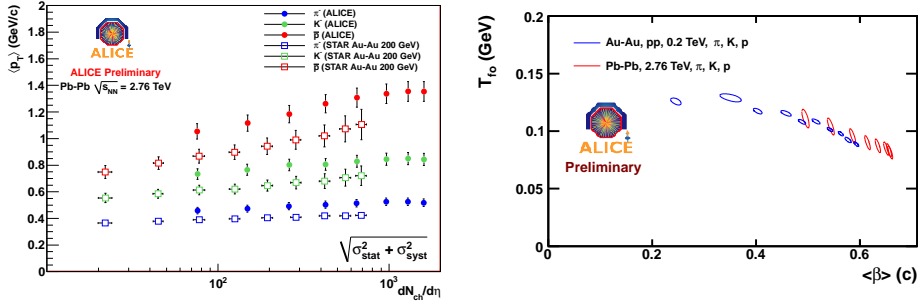


Figure 7: Hadron $\langle p_T \rangle$ as a function of the charged-particle density $dN_{ch}/d\eta$ in Pb–Pb collisions at $\sqrt{s_{NN}} = 2.76$ TeV (left). Thermal freeze-out parameters T_{fo} and $\langle \beta \rangle$ from combined blast-wave fits compared to RHIC data (right).

freeze-out temperature T_{fo} and the average transverse flow $\langle \beta \rangle$. A combined blast-wave fit of the spectra has been performed in the ranges 0.3–1.0 GeV/c, 0.2–1.5 GeV/c and 0.3–3.0 GeV/c for pions, kaons and protons respectively. While the T_{fo} parameter is slightly sensitive to the pion fit range because of feed-down of resonances the transverse flow $\langle \beta \rangle$ measurement is not, being dominated by the proton spectral shape. The results obtained on the thermal freeze-out properties in different centrality bins are compared with similar measurements performed by the STAR Collaboration at lower energies in Figure 7 (right). A stronger radial flow is observed with respect to RHIC, being about 10% larger in the most central collisions at the LHC. The data are also compared to predictions from hydrodynamic models. As already reported in [12] the pure hydrodynamic predictions [13] cannot reproduce the proton shape. A similar disagreement was observed when comparing proton elliptic flow v_2 to the same model [14]. A new calculation has been performed by U.Heinz *et al.* using a hybrid model which adds an hadronic rescattering and freeze-out stage to the pure viscous dynamics [15]. These new predictions [16] are compared to

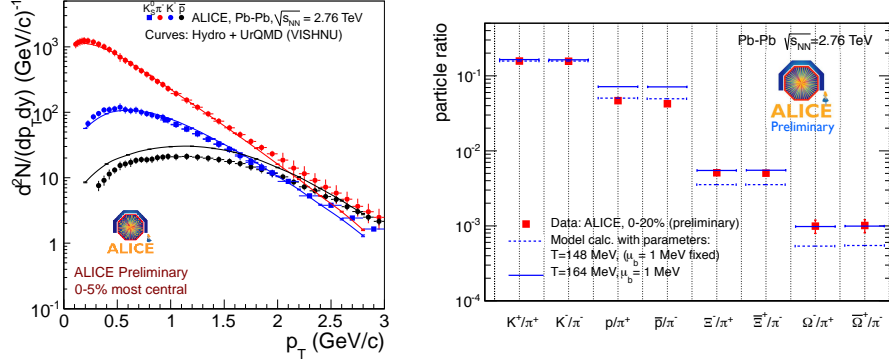


Figure 8: π^- , K^- , \bar{p} spectra in 0-5% central Pb–Pb collisions compared to hydrodynamic model predictions [15, 16] (left). Hadron-production ratios compared to thermal model predictions [11] (right).

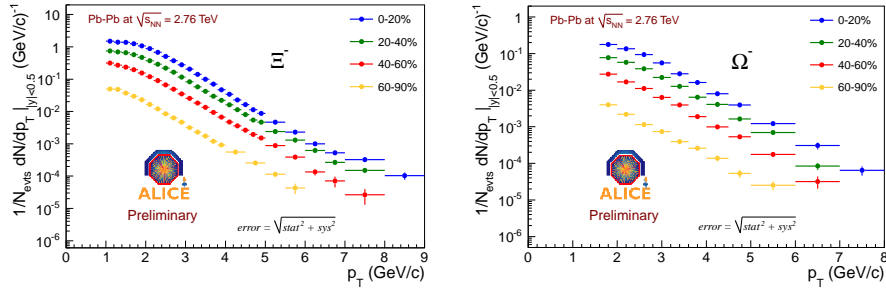


Figure 9: Transverse momentum spectra of Ξ^- (left) and Ω^- (right) measured in four centrality classes in Pb–Pb collisions at $\sqrt{s_{NN}} = 2.76$ TeV.

the data in Figure 8 (left) and the agreement with the proton shape is better than a pure hydrodynamic picture. This suggests that extra flow builds up in the hadronic phase. The difference in the proton yield can be ascribed to the fact that the model derives yields from a thermal model with $T_{ch} = 165$ MeV. It is worth that this model also reproduces the shape of elliptic flow of identified hadrons as already reported in [17].

Finally, the production of multi-strange baryons in Pb–Pb collisions has also been reported at this conference and in [18]. The transverse momentum spectra of Ξ^- and Ω^- measured in several centrality classes are shown in Figure 9. The measured yields of several hadrons normalized to the pion yield in 0-5% central collisions are compared to thermal model predictions in Figure 8 (right). With a temperature of $T_{ch} = 164$ MeV predicted by A. Andronic *et al.* [11] the model reproduces both kaon and multi-strange production but fails with protons. The same model can be tuned to reproduce proton yields with an ad-hoc $T_{ch} = 148$ MeV, though multi-strange production is underestimated in this case.

5 Conclusions

The transverse momentum spectra of π^\pm , K^\pm , p and \bar{p} have been measured with ALICE in pp collisions at $\sqrt{s} = 900$ GeV and 7 TeV and in Pb–Pb collisions at $\sqrt{s_{NN}} = 2.76$ TeV, demonstrating the excellent PID capabilities of the experiment. Proton-proton results show no evident \sqrt{s} dependence in hadron production ratios. Currently available Monte Carlo generators and tunes cannot simultaneously reproduce charge kaon and resonance production and multi-strange production is generally underestimated at low- p_T . In Pb–Pb collisions \bar{p}/π^- integrated ratio is significantly lower than statistical model predictions with a chemical freeze-out temperature $T_{ch} = 160 - 170$ MeV. The average transverse momenta and the spectral shapes indicate a $\sim 10\%$ stronger radial flow than at RHIC energies.

References

- [1] ALICE Collaboration, J. Phys. **G32**, 1295 (2006)
ALICE Collaboration, J. Instrum. **3**, S08002 (2008)
- [2] ALICE Collaboration, Eur. Phys. J. **C71**, 1655 (2011)
- [3] C. Tsallis, J. Stat. Phys. **52**, 479 (1988)
- [4] ALICE Collaboration, Phys. Rev. Lett. **105**, 072002 (2010)
- [5] A. Maire (ALICE Collaboration), Strangeness in Quark Matter 2011 conference proceedings [[hep-ex/1112.2097](#)]
- [6] STAR Collaboration, Phys. Rev. **C75**, 064901 (2007)
- [7] CMS Collaboration, JHEP **05**, 064 (2011)
- [8] ALICE Collaboration, Phys. Rev. Lett. **106**, 032301 (2011)
- [9] E. Schnedermann, J. Sollfrank and U. Heinz, Phys. Rev. **C48**, 2462 (1993)
- [10] STAR Collaboration, Phys. Rev. **C79**, 034909 (2009)
PHENIX Collaboration, Phys. Rev. **C69**, 034909 (2004)
BRAHMS Collaboration, Phys. Rev. **C72**, 014908 (2005)
- [11] J. Cleymans *et al.*, Phys. Rev. **C74**, 034903 (2006)
A. Andronic *et al.*, Phys. Lett. **B673**, 142 (2009)
- [12] M. Floris (ALICE Collaboration), Quark Matter 2011 conference proceedings [[hep-ex/1108.3257](#)]
- [13] C. Shen, U. Heinz, P. Huovinen and H. Song, [nucl-th/1105.3226](#)
- [14] R. Snellings (ALICE Collaboration), Quark Matter 2011 conference proceedings [[nucl-ex/1106.6284](#)]
- [15] U. Heinz, C. Shen, and H. Song, [nucl-th/1108.5323](#)
- [16] U. Heinz and H. Song, private communication
- [17] F. Noferini (ALICE Collaboration), Strangeness in Quark Matter 2011 conference proceedings
- [18] M. Nicassio (ALICE Collaboration), Strangeness in Quark Matter 2011 conference proceedings